Synthesis and Structure of $Pd_4(\mu\text{-}P^tBu_2)_2(\mu\text{-}CS_2)(PPh_3)_2I_2$, a Neutral Palladium(I) Derivative with a Hexacoordinate Carbon and a CS_2 Molecule Bridging Four Palladium Centers

Piero Leoni,*,† Marco Pasquali,*,‡ Luca Fadini,‡ Alberto Albinati,*,§ Peter Hofmann,*,|| and Markus Metz||

Contribution from the Scuola Normale Superiore, Piazza dei Cavalieri 7, I-56126 Pisa, Italy, Dipartimento di Chimica e Chimica Industriale, Università di Pisa, via Risorgimento 35, I-56126 Pisa, Italy, Istituto di Chimica Farmaceutica, Università di Milano, I-20131 Milano, Italy, and Organisch-Chemisches Institut, Universität Heidelberg, Im Neuenheimer Feld 270, D-69120 Heidelberg, Germany

Received January 24, 1997. Revised Manuscript Received June 20, 1997[⊗]

Abstract: The dinuclear CS_2 complex $[Pd_2(\mu\text{-}P^tBu_2)(\mu,\eta^2\text{:}\eta^2\text{-}CS_2)(PPh_3)_2]BF_4$, (**2**)$BF_4$, reacts with Me_4NI to yield the neutral tetranuclear Pd(I) derivative $Pd_4(\mu\text{-}P^tBu_2)_2(\mu_4\text{-}CS_2)(PPh_3)_2I_2$ (**4**), which has been characterized by single-crystal X-ray diffraction. Its unusual molecular structure with a formally hexacoordinate carbon atom, as well as that of $(\mathbf{2})^+$ with a planar tetracoordinate carbon can be explained on the basis of fragment MO considerations and EHMO model calculations. The reaction proceeds stepwise, with the relatively fast substitution of CS_2 by the iodide ion giving the intermediate complex $Pd_2(\mu\text{-}P^tBu_2)(\mu\text{-}I)(PPh_3)_2$ (**3**). The latter further reacts slowly with free CS_2 to give complex **4** and free PPh_3. Complex **3** was also prepared and isolated pure by reacting $[Pd_2(\mu\text{-}P^tBu_2)(PPh_3)_3]BF_4$ with Me_4NI.

Introduction

Carbon disulfide coordinates to a transition metal in a variety of modes:[1] both mononuclear complexes, where CS_2 binds the metal either η^1-end-on[2] or η^2-side-on,[3] and polynuclear derivatives have been reported.[4] Numerous types of coordination have been observed in these cases, with the CS_2 molecule *unsymmetrically* bridging di- or trimetallic moieties (Chart 1).

A common feature of these complexes is the large metal−metal separation, of nonbonded type, observed (or assumed) in structures **I** (M = Fe,[4a,b] Pd,[4h] Pt[4i,l]), **II** (M = Mo,[4m] Ni,[4c] Pd,[4d] Pt[4e]), and **III** (M = Fe[4n]), an exception being the diplatinum derivative $Pt_2(\mu,\eta^2\text{-}CS_2)(PPh_3)_4$ suggested to have the structure **IV**.[4f,g] Rare examples of CS_2 coordination to clusters of higher nuclearity are $[Co_3(CO)_9C](\mu_3\text{-}CS_2)[Co_3(CO)_7S]$, $[Co_3(CO)_8(\mu_5\text{-}CS_2)[Co_3(CO)_7S]$,[4o] and $[Co_8(CO)_{21}(\mu\text{-}CS_2)(\mu\text{-}C_2S)]$.[4p]

We have recently reported[5] (see Scheme 1) the reversible reaction of $[Pd_2(\mu\text{-}P^tBu_2)(PPh_3)_3]BF_4$, (**1**)$BF_4$, with CS_2, yielding the dinuclear palladium(I) derivative $[Pd_2(\mu\text{-}P^tBu_2)(\mu,\eta^2\text{:}\eta^2\text{-}CS_2)(PPh_3)_2]BF_4$, (**2**)$BF_4$, with the carbon disulfide molecule forming a planar and *symmetrical* $Pd_2(\mu\text{-}CS_2)$ core, with *planar tetracoordinate* carbon. Here we describe the synthesis and crystal and molecular structure of $Pd_4(\mu\text{-}P^tBu_2)_2(\mu_4\text{-}CS_2)(PPh_3)_2I_2$, (**4**); the CS_2 molecule exhibits an unprecedented coordination mode in this complex, with *hexacoordinate* carbon. The structures of cation $(\mathbf{2})^+$ and of complex **4** were explained by a theoretical study based on extended Hückel molecular orbital calculations.

Chart 1

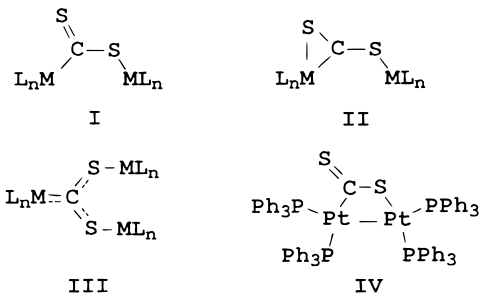

† Scuola Normale Superiore.
‡ Università di Pisa.
§ Università di Milano.
|| Universität Heidelberg.
⊗ Abstract published in *Advance ACS Abstracts,* August 1, 1997.

(1) (a) Pandey, K. K. *Coord. Chem. Rev.* **1995**, *140*, 37. (b) Ibers, J. A. *Chem. Soc. Rev.* **1982**, *11*, 57. (c) Werner, H. *Coord. Chem. Rev.* **1982**, *43*, 165.

(2) (a) Lee, G. R.; Maher, J. M.; Rooper, N. J. *J. Am. Chem. Soc.* **1987**, *109*, 2956. (b) Angelici, R. J.; Dunker, J. W. *Inorg. Chem.* **1985**, *24*, 2215. (c) Ruiz-Ramirez, L.; Stephenson, T. A.; Switkes, E. S. *J. Chem. Soc., Dalton Trans.* **1973**, 1770. (d) Moers, F. G.; ten Hoedt, R. W. M.; Langhout, J. P. *Inorg. Chem.* **1973,** *12*, 2196. (e) Yagupski, M. P.; Wilkinson, G. *J. Chem. Soc. (A)* **1968**, 2813. (f) Biard, M. C.; Wilkinson, G. *J. Chem. Soc. (A)* **1967**, 865. (g) Brown, D.; Hughes, F. *Inorg. Chim. Acta* **1967**, *1*, 448

(3) (a) Werner, H.; Ebner. M.; Bertleff, W. *Z. Naturforsch.* **1985**, *40b*, 1351. (b) Bianchini, C.; Mealli, C.; Meli, A.; Sabat, M.; Zanello, P. *J. Am. Chem. Soc.* **1987**, *109*, 185. (c) Bianchini, C.; Meli, A.; Scapacci, G. *Organometallics* **1983**, *2*, 1834. (d) Heberhold, M.; Hill, A. F.; McAuley, N.; Roper, W. R. *J. Organomet. Chem.* **1986**, *310*, 95. (e) Gaffney, T. R.; Ibers, J. A. *Inorg. Chem.* **1982**, *21*, 2851. (f) Alt, H. G.; Schwind, K.-H., Rausch, M. D. *J. Organomet. Chem.* **1987**, *321*, C9.

(4) (a) Stolzenberg, H.; Fehlhammer, W. P.; Monari, M.; Zanotti, V.; Busetto, L. *J. Organomet. Chem.* **1984**, *272*, 73. (b) Derry, M. E. G.; Landrum, B. E.; Shibley, J. L.; Cutler, A. R. *J. Organomet. Chem.* **1989**, *378*, 421. (c) Bianchini, C.; Ghilardi, S. A.; Meli, A.; Midollini, S.; Orlandini, A. *J. Chem. Soc., Chem. Commun.* **1983**, 753. (d) Farrar, D. H.; Gukathasan, R. R.; Won, K. *J. Organomet. Chem.* **1984**, *275*, 263. (e) Farrar, G. H.; Gukathasan, R. R.; Morris, S. A. *Inorg. Chem.* **1984**, *23*, 3258. (f) Ma, E.; Semelhago, G.; Walker, W.; Farrar, D. H.; Gukathasan, R. R. *J. Chem. Soc., Dalton Trans.* **1985**, 2595. (g) Ebner, M.; Otto, H.; Werner, H. *Angew. Chem., Int. Ed. Engl.* **1985**, *24*, 518. (h) Kullberg, M. L.; Kubiak, C. P. *Inorg. Chem.* **1986**, *25*, 26. (i) Langrick, C. R.; Pringle, P. G.; Shaw, B. L. *J. Chem. Soc., Dalton Trans.* **1985**, 1015. (l) Cameron, T. S.; Gardner, P. A.; Brundy, K. R. *J. Organomet. Chem.* **1981**, *212*, C19. (m) Deutsch, W.; Gieren, A.; Ruiz-Perez, C.; Schwarzhaus, K. E. *J. Organomet. Chem.* **1988**, *355*, 197. (n) Busetto, L.; Monari, M.; Palazzi, A.; Albano, V.; Demartin, F. *J. Chem. Soc., Dalton Trans.* **1983**, 1849. (o) Gervasio, G.; Rossetti, R.; Stanghellini, P. L.; Bor, G. *Inorg. Chem.* **1982**, *21*, 3781. (p) Gervasio, G.; Rossetti, R.; Stanghellini, P. L.; Bor, G. *J. Chem. Soc., Dalton Trans.* **1987**, 1707.

(5) Leoni, P.; Pasquali, M.; Pieri, G.; Albinati, A.; Pregosin, P. S.; Rüegger, H. *Organometallics* **1995**, *14*, 3143.

S0002-7863(97)00262-X CCC: $14.00

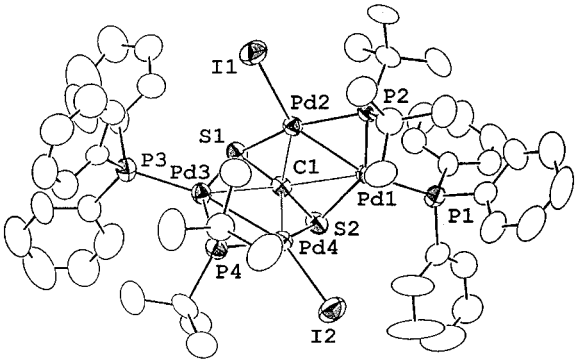

Figure 1. ORTEP diagram of **4**. Hydrogens were omitted for clarity.

Scheme 1

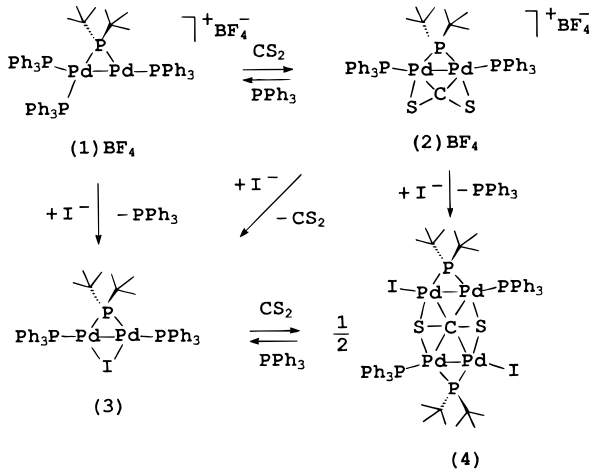

Table 1. Selected Interatomic Distances (Å) and Bond Angles (deg) for (**4**)·CH_2Cl_2

Pd1−Pd2	2.6820(8)	I1−Pd2−Pd1	151.24(3)
Pd3−Pd4	2.6725(9)	I2−Pd4−Pd3	150.27(3)
Pd1−S2	2.342(2)	I1−Pd2−S1	105.76(6)
Pd1−P1	2.296(2)	I1−Pd2−C1	145.9(2)
Pd1−P2	2.239(2)	I2−Pd4−S2	105.35(7)
Pd2−P2	2.282(2)	I2−Pd4−C1	145.5(2)
Pd3−P3	2.286(2)	P1−Pd1−P2	114.26(8)
Pd3−P4	2.242(2)	P1−Pd1−S2	103.19(8)
Pd4−P4	2.292(2)	P3−Pd3−P4	115.10(9)
Pd2−C1	2.114(7)	P3−Pd3−S1	102.94(9)
Pd1−C1	2.549(8)	I1−Pd2−P2	98.52(6)
Pd4−C1	2.101(8)	Pd1−P2−Pd2	72.77(6)
Pd2−S1	2.439(2)	I2−Pd4−P4	97.62(7)
Pd3−S1	2.340(2)	Pd3−P4−Pd4	72.22(7)
Pd4−S2	2.442(2)	S1−C1−S2	134.6(5)
I1−Pd2	2.6362(9)	Pd2−S1−Pd3	86.55(7)
I2−Pd4	2.6229(9)	Pd1−S2−Pd4	87.59(8)
S2−C1	1.714(8)	S1−Pd2−C1	43.8(2)
S1−C1	1.724(9)	Pd2−C1−Pd4	106.3(3)

Results and Discussion

When a yellow acetone solution of complex (**2**)BF_4 was reacted with a stoichiometric amount of Me_4NI, its color turned quickly deep green. On standing for a few hours, a red microcrystalline solid precipitated out and the green color of the solution disappeared. The red solid was isolated and characterized by IR, NMR, and single-crystal X-ray diffraction.

An ORTEP view of the structure is given in Figure 1, and significant bond distances and angles are listed in Table 1.

The structure consists of two "$(PPh_3)Pd(\mu\text{-}P^tBu_2)PdI$" units joined together by a CS_2 molecule coordinated, via the sulfurs and the central carbon atom, to the four palladium atoms and resulting in a butterfly geometry for the complex; the dihedral angle between the least-squares planes defined by the atoms Pd1, Pd2, P1, P2 and Pd3, Pd4, P3, P4, respectively, is ca. 94°. For clarity, two different views of the $[PPd(\mu\text{-}P)PdI]_2(\mu\text{-}CS_2)$ core alone are shown in Figure 2.

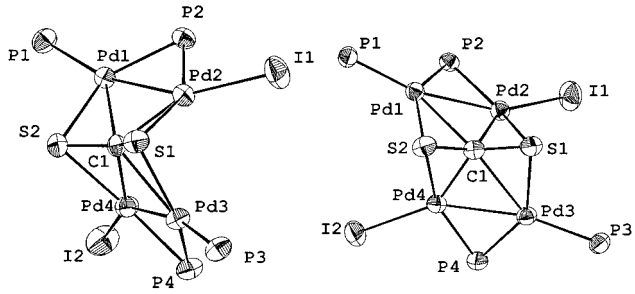

Figure 2. Two different views of the $[PPd(\mu\text{-}P)PdI]_2(\mu\text{-}CS_2)$ core of complex **4** (all organic groups were omitted for clarity).

The molecular geometries of both cation $(\mathbf{2})^+$ and of the neutral complex **4** can be readily understood on the basis of the bonding capability and electronic requirements of a general $[L_2Pd_2(\mu\text{-}X)]$ fragment with two Pd(I) centers. The electronic structure of such building blocks has been detailed before.[6] Their main feature for an overall d^9-d^9 electron count, practically irrespective of the bridging group μ-X (anions such as halide, allyl, Cp, carboxylate, sulfide, phosphide, etc., or neutral molecules such as bisphosphines, butadiene, benzene, etc., all acting as formal four-electron (4e) donors) and independent of the terminal 2e donor ligands L (in most cases phosphines, but also anions as I^- in **4**) is the availability at low energy of two empty MOs above a nest of nine filled d levels. These two acceptor levels ($1b_2$ and $2a_1$) and the highest filled orbital ($1a_1$), as they evolve from EH calculations for the simplified moiety $[(PH_3)_2Pd_2(\mu\text{-}PH_2)]^+$, which we have used for modeling cation $(\mathbf{2})^+$ as $[(PH_3)_2Pd_2(\mu\text{-}PH_2)(\mu,\eta^2\text{:}\eta^2\text{-}CS_2)]^+$, are sketched qualitatively in **5**.[7]

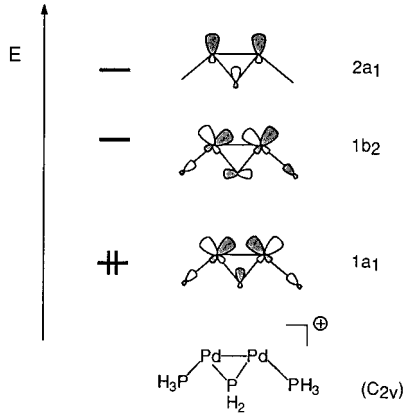

5

As observed experimentally for $(\mathbf{2})^+$ and **4** and for other unsymmetrical systems $[L_2Pd_2(\mu\text{-}X)(\mu\text{-}Y)]$, the two terminal ligands often bend toward one of the two bridging ligands (μ-P^tBu_2), optimizing the interaction with the other (CS_2).[8] Due to its frontier orbitals displayed in **5**, a single fragment $[(PH_3)_2$-

(6) (a) The first analysis of electronic structures and bonding in ligand bridged dinuclear d^9-d^9 complexes $[L_2Pd_2(\mu\text{-}X)(\mu\text{-}Y)]$, carried out by one of the present authors, can be found in: Werner, H. *Adv. Organomet. Chem.* **1981**, *19*, 155. (b) Zhu, L.; Kostic, N. M. *Organometallics* **1988**, *7*, 665. (c) Ogoshi, S.; Tsutsumi, K.; Ooi, M.; Kurosawa, H. *J. Am. Chem. Soc.* **1995**, *117*, 10415. (d) Kurosawa, H.; Hirako, K.; Natsume, S.; Ogoshi, S.; Kanehisa, N.; Kai, Y. *Organometallics* **1996**, *15*, 2089.

(7) The geometry of **5** with Pd−Pd−P angles of 152° was taken from the partially optimized structure of $[Pd_4(\mu\text{-}PH_2)_2(\mu_4\text{−}CS_2)(PH_3)_4]^{2+}$ (see below).

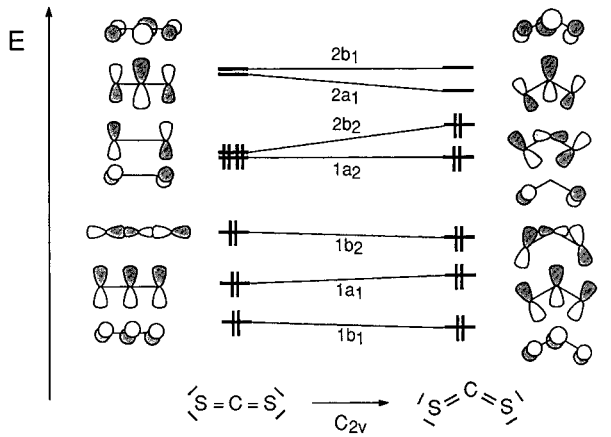

Figure 3. Qualitative Walsh diagram for bending CS_2 (EH).

$Pd_2(\mu\text{-}PH_2)]^+$ and its real analogue $[(PPh_3)_2Pd_2(\mu\text{-}P^tBu_2)]^+$ in $(\mathbf{2})^+$ formally are 4e acceptors. They are suited to interact with a bent CS_2 molecule in precisely the coplanar arrangement of the Pd_2P and CS_2 plane (creating a planar, tetracoordinate carbon atom[9]) of the molecular geometry of cation $(\mathbf{2})^+$.[5] As represented in the Walsh-type diagram of Figure 3, adopting a bent structure prepares CS_2 for optimal bonding to the Pd_2 unit: the carbon disulfide HOMO $2b_2$ interacts strongly with the LUMO $1b_2$ of the metal fragment, the upper empty level $2a_1$ of the latter overlaps with $1a_1$ of CS_2, and some back-bonding to the organic ligand occurs by interaction of its LUMO $2a_1$ with the HOMO $1a_1$ of $[(PH_3)_2Pd_2(\mu\text{-}PH_2)]^+$.

In the neutral cluster compound **4**, two dinuclear metal fragments $[Pd_2(\mu\text{-}P^tBu_2)(PPh_3)I]$ are bound to one CS_2. In our calculations we used $[Pd_4(\mu\text{-}PH_2)_2(\mu_4\text{-}CS_2)(PH_3)_4]^{2+}$ as a symmetric model for cluster **4**, employing two $[(PH_3)_2Pd_2(\mu\text{-}PH_2)]^+$ fragments as dipalladium units.[10] To satisfy the electron demand for both of them, they have to coordinate to both faces of a bent CS_2, aligning their orbital lobes and thus their $Pd_2(\mu\text{-}P)$ planes for maximum overlap. Partial optimization of the position and orientation of two $[(PH_3)_2Pd_2(\mu\text{-}PH_2)]^+$ fragments[11] above and below the bent CS_2 yields a structure nearly superimposable to that observed in the X-ray study (two different views of the partially optimized geometry, oriented as in Figure 2, for $[Pd_4(\mu\text{-}PH_2)_2(\mu_4\text{-}CS_2)(PH_3)_4]^{2+}$ as a model of **4** are shown in Figure S2 of the Supporting Information), the lower symmetry of **4** (vide infra) is a consequence of its unsymmetric, mixed PPh_3/I terminal ligand set. Only with bent CS_2 in a "sandwiched" position does each of the six possible symmetry-adapted linear combinations derived from the frontier orbitals (viz. **5**) of the two dipalladium units find a partner of appropriate symmetry and overlap within the set of valence MOs of Figure 3. Four occupied levels ($2b_2$, $1b_1$, $1a_2$, and $1a_1$) of CS_2, holding a total of eight electrons, are used for donation to the metal acceptor MOs, and the LUMOs $2a_1$ and $2b_1$ of CS_2 provide the correct nodal character to accept electron density from the two metal $1a_1$ linear combinations and are responsible for back-bonding to CS_2. Therefore, in $(\mathbf{2})^+$ and in **4**, metal to CS_2 bonding is established from both Pd atoms of each Pd_2 subunit *to carbon and to the sulfur centers*, of course—unlike in our model $[Pd_4(\mu\text{-}PH_2)_2(\mu_4\text{-}CS_2)(PH_3)_4]^{2+}$—to a different extent in the unsymmetrical real molecule **4**.

Experimentally, the two Pd−Pd separations in **4** (2.6820(8) and 2.6725(9) Å, respectively) are shorter than that found in complex $(\mathbf{2})^+$ (2.708(1) Å).[5] As expected, the Pd−S distances are different, each Pd_2 moiety being similarly coordinated via one short and one long bond: Pd1−S2 2.342(2), Pd2−S1 2.439(2), Pd3−S1 2.340(2), and Pd4−S2 2.442(2) Å, respectively. Moreover these distances are equal two by two, and two of them are longer than those found in the cation $(\mathbf{2})^+$ (av 2.341(3) Å).[5] It may be noted that the phosphido bridge is also asymmetric (Pd−P_{av} 2.241(2) and 2.287(5) Å, respectively) with the shorter distance being trans to the longer Pd−S separation, reflecting the different bonding modes of the sulfur donor centers to the left/right unsymmetric metal units. As found for the Pd−S distances, there are two sets of Pd−C bonds, one set shorter and the other one longer than the Pd−S bonds [Pd2−C1 = 2.114(7) and Pd4−C1 = 2.101(8) Å; Pd1−C1 = 2.549(8) and Pd3−C1 = 2.584(8) Å]. These geometric details are of course not reproduced by the calculations because of the C_{2v} symmetry of the model system $[Pd_4(\mu\text{-}PH_2)_2(\mu_4\text{-}CS_2)(PH_3)_4]^{2+}$ (see the Experimental Section). The two C−S separations of **4** are at 1.719 (7) Å (av) and longer than in $(\mathbf{2})^+$ (av 1.612(8) Å) as expected from the 8e vs 4e donor nature of CS_2 in **4** and $(\mathbf{2})^+$. This fact is also reflected in the S1−C1−S2 angle of 134.6 (5)°, more acute than in $(\mathbf{2})^+$ (145°).[5]

The butterfly structure of the solid state is retained in solution: ^1H and $^{13}C\{^1H\}$ NMR spectra exhibit two different signals for the nuclei of the *tert*-butyl substituents on the bridging phosphides (see the Experimental Section) and, therefore, clearly show their unequivalence. It is also worth noticing the large highfield shift for C1 (δ = 117 ppm) with respect to the corresponding carbon of the cation $(\mathbf{2})^+$ (212 ppm).

The transient appearance of the green color in the early steps of the preparation of complex **4** is due to the formation of the intermediate compound $[Pd_2(\mu\text{-}P^tBu_2)(\mu\text{-}I)(PPh_3)_2]$, **3**, which arises from the substitution, by the iodide ion, of the bridging CS_2 molecule of $(\mathbf{2})BF_4$. If CS_2 is evacuated from the flask, **3** can be isolated in good yield. However, if not removed immediately, carbon disulfide reacts slowly with **3** (see Scheme 1), giving the thermodynamically favored complex **4** and free PPh_3; the last reaction shows full reversibility, and complex **3** is reformed quantitatively by adding an excess of PPh_3 to a toluene solution of **4**.

Complex **3** has also been prepared by an independent route, i.e., by reacting $(\mathbf{1})BF_4$ with Me_4NI; its structure was straightforwardly inferred from elemental and spectroscopic analyses. Two signals were in fact observed in the $^{31}P\{^1H\}$ NMR spectrum, at 443.5 ppm (triplet, $^2J_{PP}$ = 85 Hz), for the bridging phosphorus, and at 34.3 ppm (doublet, $^2J_{PP}$ = 85 Hz), for the two equivalent phosphines. As confirmed by a molecular weight determination (cryoscopy in C_6H_6), complex **3** is a dinuclear derivative and not a major oligomer.

Finally, it should be mentioned that the rare hexacoordinated carbon atoms previously known are generally interstitial compounds, with an isolated carbon atom buried in the metal center's

(8) Bending the two terminal ligands of a d^9-d^9 $[L_2Pd_2(\mu\text{-}X)]$ fragment toward X, as shown in **5**, serves to improve overlap and bonding to a second bridging ligand by rehybridization and by orbital energy shifts due to the geometric distortion. In addition, steric repulsion with the larger bridging group is reduced.

(9) (a) Hoffmann, R.; Alder, R. W.; Wilcox, C. F., Jr. *J. Am. Chem. Soc.* **1970**, *92*, 4992. (b) Another beautiful, most recent example of planar, tetracoordinate carbon in an organometallic compound has just been reported: Hyla-Kryspin, I.; Gleiter, R.; Rohmer M.-M.; Devemy J.; Gunale, A.; Pritzkow, H.; Siebert, W. *Chem. Eur. J.* **1997**, *3*, 294.

(10) We also performed EH calculations for the unsymmetrical, neutral model system $[Pd_4(\mu\text{-}PH_2)_2(\mu_4\text{-}CS_2)(PH_3)_2Cl_2]$, using Cl^- instead of I^- as terminal ligands because of more reliable EH atomic parameters for Cl. The general bonding pattern described for the symmetric system remains unaffected.

(11) The Pd−Pd−PH_3 angles within the $[(PH_3)_2Pd_2(\mu\text{-}PH_2)]^+$ subunits as well as their distances and the relative orientations of their $Pd_2P_2(\mu\text{-}P)$ planes with respect to the plane of the bent CS_2 unit were optimized independently. During the optimization overall C_{2v} symmetry was retained, and except for the Pd−Pd−P angles, the CS_2 and $[(PH_3)_2Pd_2(\mu\text{-}PH_2)]^+$ subunits were kept at frozen model geometries, adapted from the X-ray structure of **4**. For details see the Experimental Section.

cage.[12] In complex **4,** the carbon atom is bonded to four metal centers and still binds the two sulfur atoms. In this way the CS_2 molecule retains its identity and, as shown above and despite the hexacoordination, can be easily removed from the coordination pocket.

Experimental Section

General Procedures. All preparations were performed under a nitrogen atmosphere using standard Schlenk techniques. Solvents were refluxed under nitrogen several hours over suitable drying agents and freshly distilled under nitrogen prior to use. Deuterated solvents were used without further purification but were deoxygenated by freeze−pump−thaw cycles and stored under nitrogen on molecular sieves. $[Pd_2(\mu\text{-}P^tBu_2)(PPh_3)_3]BF_4$, (**1**)$BF_4$,[5] and $[Pd_2(\mu\text{-}P^tBu_2)(\mu,\eta^2{:}\eta^2\text{-}CS_2)(PPh_3)_2]BF_4$, (**2**)$BF_4$,[5] were prepared by the previously reported procedures. CS_2 (Aldrich), $^{13}CS_2$ (Cambridge Isotope Labs), PPh_3 (Aldrich), and Me_4NI (Aldrich) were used as purchased.

IR spectra (Nujol mulls, KBr) were recorded on a Perkin-Elmer FT-IR 1725X spectrophotometer. NMR spectra were recorded on a Varian Gemini 200 BB instrument; frequencies are referenced to the residual signal of the deuterated solvent (^1H, ^{13}C) or to external 85% H_3PO_4 (^{31}P, the shifts downfield from the reference being considered as positive).

Preparation of $[Pd_2(\mu\text{-}P^tBu_2)(\mu\text{-}I)(PPh_3)_2]$ (3). A red solution of (**1**)BF_4 (297 mg, 0.241 mmol) in acetone (10 mL) turned immediately deep green upon the addition of Me_4NI (58 mg, 0.289 mmol). The mixture was stirred for 15 min at room temperature, and the solvent was evaporated. The residue was dissolved in toluene (20 mL) and filtered. A green microcrystalline solid precipitated out by the addition of *n*-hexane (20 mL), and the suspension was kept 12 h at −20 °C and filtered; the solid was washed twice with *n*-hexane (5 mL) and *vacuum* dried (229 mg, 94.1%). Elemental Anal. Calcd for $C_{44}H_{48}IP_3Pd_2$: C, 52.4; H, 4.80. Found: C, 52.1; H, 4.75. IR (Nujol, KBr): 3040 ($\nu_{=CH}$), 1572, 1494 ($\nu_{C=C}$) cm^{-1}. NMR (C_6D_6, 293 K): $^{31}P\{^1H\}$ δ (ppm) 443.5 (t, $^2J_{PP}$ = 85 Hz, μ-*P*), 34.3 (d, $^2J_{PP}$ = 85 Hz, *P*Ph_3); ^1H δ (ppm) 7.96 (m, 12 H), 7.02 (m, 18 H), 1.03 (d, $^3J_{PH}$ = 13 Hz, 18H, C*H*$_3$). Molecular weight: 1039 (by cryoscopy in C_6H_6).

Preparation of $Pd_4(\mu\text{-}P^tBu_2)_2(\mu_4\text{-}CS_2)(PPh_3)_2I_2$ (4). Method a: An acetone (5 mL) solution of Me_4NI (56 mg, 0.278 mmol) was dropped into a yellow solution of (**2**)BF_4 (261 mg, 0.250 mmol) in acetone (5 mL). The color of the solution turned deep green in a few minutes. The $^{31}P\{^1H\}$ NMR spectrum of a small sample of the solution exhibited the resonances described above, due to complex **3**, and of uncoordinated PPh_3 as the only P-containing species in solution. Leaving the solution at room temperature, a gradual variation of its color to red was observed, with the precipitation of a red solid. After 6 h, the solvent was evaporated and the residue dissolved in toluene (10 mL). A white solid was filtered off, and the red solution was concentrated to ca. one-half of the starting volume. By adding *n*-hexane (10 mL) to the filtrate, a red solid precipitated out and was filtered, washed twice with *n*-hexane (3 mL), and *vacuum* dried (160 mg, 81.5% yield). Elemental Anal. Calcd for $C_{53}H_{66}I_2P_4Pd_4S_2$: C, 40.6; H, 4.24. Found: C, 40.4; H, 4.21. IR (Nujol, KBr): 3040 ($\nu_{=CH}$), 1494, 1456 ($\nu_{C=C}$), 1098 (ν_{CS}) cm^{-1}. NMR ($CDCl_3$, 293 K): $^{31}P\{^1H\}$ δ (ppm) 403.2 (d, $^2J_{PP}$ = 36 Hz, μ-*P*), 23.8 (d, $^2J_{PP}$ = 36 Hz, *P*Ph_3); ^1H δ (ppm) 7.8 (m, 12 H), 7.45 (m, 18H), 1.17 (d, $^3J_{PH}$ = 18 Hz, C*H*$_3$), 1.13 (d, $^3J_{PH}$ = 14 Hz, C*H*$_3$); $^{13}C\{^1H\}$ δ (ppm) 134.4 (d, $^2J_{CP}$ = 12 Hz, C_{ortho}), 133.5 (d, $^2J_{CP}$ = 42 Hz, C_{ipso}), 130.4 (s, C_{para}), 128.7 (d, $^3J_{CP}$ = 7 Hz, C_{meta}), 117.1 (s, *C*S_2), 42.9 (br s, *C*Me_3), 33.0 (br s, *C*H_3), 31.7 (br s, *C*H_3).

Method b: CS_2 (10 μL, 0.166 mmol) was added to a deep green toluene (5 mL) solution of complex **3** (124 mg, 0.123 mmol). The color of the solution turned red in a few minutes, and a red solid started to precipitate. The suspension was stirred for 2 h at room temperature and was kept, after the addition of Et_2O (5 mL), for 12 h at −20 °C. The solid was filtered, washed twice with *n*-hexane (3 mL), and *vacuum* dried (65 mg, 67.3% yield). Single crystals for the crystal structure determination were obtained by recrystallization from CH_2Cl_2/Et_2O mixtures. IR and NMR spectra of the sample were undistinguishable from those described above for the sample obtained with method a).

By the same procedure of method b, starting from $^{13}CS_2$, we prepared the labeled $Pd_4(\mu\text{-}P^tBu_2)_2(\mu_4\text{-}^{13}CS_2)(PPh_3)_2I_2$, (**4***). NMR ($CDCl_3$, 293 K): $^{31}P\{^1H\}$ δ (ppm) 403.2 (br d, $^2J_{PP}$ = 36 Hz, μ-*P*), 23.8 (dd, $^2J_{PP}$ = 36 Hz, $^2J_{PC}$ = 14 Hz, *P*Ph_3); $^{13}C\{^1H\}$ δ (ppm) 134.5 (d, $^2J_{CP}$ = 12 Hz, C_{ortho}), 133.1 (d, $^1J_{CP}$ = 42 Hz, C_{ipso}), 130.5 (br s, C_{para}), 128.7 (d, $^3J_{CP}$ = 7 Hz, C_{meta}), 117.1 (br t, J_{CP} = 14 Hz, CS_2), 42.9 (br s, *C*Me_3), 33.0 (br s, *C*H_3), 31.7 (br s, *C*H_3).

Molecular Orbital Calculations. The molecular orbital calculations are of the extended Hückel type.[13] A modified Wolfsberg−Helmholtz formula is employed for the calculation of H_{ij} matrix elements.[14] The atomic parameters (wave functions, valence state ionization energies) used for C and H are standard ones; those for S[15] and P[16] have been taken from earlier work. For Pd the following set of atomic parameters from an earlier SCC calculation of $[Pd_2(PH_3)_2(\mu\text{-allyl})(\mu\text{-Cp})]$ (ref 6a) was used: Pd 5s, ζ = 2.190, H_{ii} = −7.680 eV; Pd 5p, ζ = 2.152, H_{ii} = −4.050 eV; Pd 4d, ζ_1 = 5.983, c_1 = 0.5535, ζ_2 = 2.613, c_2 = 0.6701, H_{ii} = −12.51 eV. The following geometric parameters were used in our MO calculations for **5** and the corresponding fragments $[(PH_3)_2Pd_2(\mu\text{-}PH_2)]^+$ in the symmetric model $[Pd_4(\mu\text{-}PH_2)_2(\mu_4\text{-}CS_2)(PH_3)_4]^{2+}$ of **4**: C_{2v} symmetry; distances Pd−Pd = 2.650 Å, Pd−P = 2.300 Å, Pd−μP = 2.260 Å, P−H = 1.420 Å; Pd−μP−Pd = 71.79°, Pd−P−H = 109.45°, Pd−μP−H = 116.94°, H−μP−H = 112.0°; free CS_2: C−S = 1.610 Å; CS_2 in $[Pd_4(\mu\text{-}PH_2)_2(\mu_4\text{-}CS_2)(PH_3)_4]^{2+}$: C−S = 1.716 Å, S−C−S = 135.0°. The related parameters in our partially optimized model $[Pd_4(\mu\text{-}PH_2)_2(\mu_4\text{-}CS_2)(PH_3)_4]^{2+}$ are Pd−C = 2.174 Å, Pd−S = 2.032 Å, and Pd−Pd−P = 152°. Note that due to well−known inability of the extended Hückel method to accurately calculate bond distances no attempts were made to optimize the geometry of the model $[Pd_4(\mu\text{-}PH_2)_2(\mu_4\text{-}CS_2)(PH_3)_4]^{2+}$ any further.

Crystallography. A suitable crystal was mounted, on a glass fiber, on a CAD4 diffractometer and was used for the space group determination and for the data collection. Unit cell dimensions were obtained by least-squares fit of the 2θ values of 25 high-order reflections (9.78 ≤ θ ≤ 18.18°). Selected crystallographic and other relevant data are listed in Table 2 and Table S1 of the Supporting Information.

Data were measured with variable scan speed to ensure constant statistical precision on the collected intensities. Three standard

Table 2. Crystallographic and Experimental Data for the X-ray Diffraction Study of (**4**)·CH_2Cl_2

formula	$C_{54}H_{68}Cl_2I_2P_4Pd_4S_2$
fw	1655.48
crystal dimens, mm	0.30 × 0.20 × 0.20
data colln *T*, °C	23
cryst syst	orthorombic
space group	*Pna*2$_1$
a, Å	21.221(8)
b, Å	17.916(2)
c, Å	16.526(2)
V, Å^3	6283(1)
Z	4
ρ (calcd), g cm^{-3}	1.750
radiation	Mo Kα (graphite monochromated λ = 0.710 69 Å)
μ, cm^{-1}	23.681
transmission coeff	1.206−0.849
θ range, deg	2.5 < θ < 27.0
no. of obsd reflns (n_o) ($\|F_o\| > 3.0\sigma(\|F\|)$)	6453
R^a	0.034
$R_w{}^a$	0.046
GOF	2.177

[a] $R = \sum(|F_o - (1/k)F_c|)/\sum|F_o|$; $R_w = [\sum_w(F_o - (1/k)F_c)^2/\sum_w|F_o|^2]^{1/2}$, where $w = [\sigma^2(F_o)]^{-1}$, $\sigma(F_o) = [\sigma^2(F_o{}^2) + f^4(F_o{}^2)]^{1/2}/2F_o$, and f = 0.03.

(12) (a) Bradley, J. S. *Adv. Organomet. Chem.* **1983**, *22*, 1. (b) Scherbaum, F.; Grohmann, A.; Huber, G.; Krüger, Schmidbaur, H. *Angew. Chem., Int. Ed. Engl.* **1988**, *27*, 1544.

(13) Hoffmann, R. *J. Chem. Phys.* **1963**, *39*, 1379.

(14) Ammeter, J. H.; Bürgi, H. B.; Tibeault, J. C.; Hoffmann, R. *J. Am. Chem. Soc.* **1978**, *100*, 3886.

(15) Pinhas, A. R.; Hoffmann, R. *Inorg. Chem.* **1979**, *18*, 654.

(16) Hofmann, P.; Hämmerle, M.; Unfried, G. *New. J. Chem.* **1991**, *15*, 769.

reflections were used to check the stability of the crystal and of the experimental conditions and measured every hour: a decay of the standards, of approximately 8%, was observed. Data were corrected for Lorentz and polarization factors using the data reduction programs of the MOLEN crystallographic package.[17] An anisotropic decay correction as well as an empirical absorption correction were also applied (azimuthal (Ψ) scans of four reflections having $\chi > 88°$).[18] The standard deviations on intensities were calculated in terms of statistics alone, while those on F_o were calculated as shown in Table 2.

The structure was solved by a combination of Patterson and Fourier methods and refined by full-matrix least squares. During the refinement, a Fourier difference map revealed the presence of a chlathrated solvent molecule (CH_2Cl_2), that was included in the refinement. Anisotropic displacement parameters were used for all atoms, except the slightly disordered solvent molecule that was refined isotropically (an anisotropic model for this molecule did not give any statistically significant improvement).[19]

As can be judged from their large displacement parameters, few carbon atoms are disordered (e.g., C332 and C333) but no meaningful model could be constructed.

The function minimized was $[\sum_w(F_o - (1/k)F_c)^2])$ with $w = [\sigma^2(F_o)]^{-1}$. No extinction correction was deemed necessary. The scattering factors used, corrected for the real and imaginary parts of the anomalous dispersion, were taken from the literature.[20] The contribution of the hydrogen atoms in their calculated positions (C−H = 0.95 Å) was taken into account but not refined.

The handedness of the structure was tested by refining both enantiomorphs; the coordinates giving the significantly[19] lower R_w factor were used and are listed in Table S2 of the Supporting Information. Upon convergence the final Fourier difference map showed no significant peaks. All calculations were carried out by using the Enraf-Nonius MOLEN crystallographic programs.[17]

Acknowledgment. This paper is dedicated to Prof. R. Gleiter on the occasion of his 60th birthday. Financial support from the CNR, Rome, and the Ministero dell'Università e della Ricerca Scientifica e Tecnologica (MURST) is gratefully acknowledged. The work at Heidelberg was generously supported by a Kekulé Grant of the Fonds der Chemischen Industrie to M.M.

Supporting Information Available: Tables of crystallographic and X-ray experimental data, final positional and isotropic equivalent displacement parameters, calculated hydrogen positions, anisotropic displacement parameters, bond distances, bond angles, and torsion angles, an ORTEP view of the molecule showing the full numbering scheme, and views of the partially optimized geometry of $[Pd_4(\mu\text{-}PH_2)_2(\mu_4\text{-}CS_2)(PH_3)_4]^{2+}$ as a model of **4** (16 pages). See any current masthead page for ordering and Internet access instructions.

JA970262+

(17) *MOLEN* Enraf-Nonius Structure Determination Package; Enraf-Nonius: Delft, The Netherlands, 1990.

(18) North, A. C. T.; Phillips, D. C.; Mathews, F. S. *Acta Crystallogr., Sect. A* **1968**, *24*, 351.

(19) Hamilton, W. C. *Acta Cristallogr.* **1965**, *17*, 502.

(20) *International Tables for X-ray Crystallography*; Kynoch: Birmingham, England, 1974; Vol. IV.